

# Low-optical-loss, low-resistance Ag/Ge based ohmic contacts to n-type InP for membrane based waveguide devices

L. Shen,<sup>1,\*</sup> V. Dolores-Calzadilla,<sup>1</sup> C.W.H.A. Wullems,<sup>1</sup> Y. Jiao,<sup>1</sup> A. Millan-Mejia,<sup>1</sup> A. Higuera-Rodriguez,<sup>1</sup> D. Heiss,<sup>1</sup> J.J.G.M. van der Tol,<sup>1</sup> H.P.M.M. Ambrosius,<sup>1</sup> G. Roelkens,<sup>1,2</sup> and M.K. Smit,<sup>1</sup>

<sup>1</sup>Photonic Integration Group, Eindhoven University of Technology, 5600 MB Eindhoven, The Netherlands

<sup>2</sup>Photonics Research Group, Ghent University-IMEC, B-9000 Ghent, Belgium

\*[l.shen@tue.nl](mailto:l.shen@tue.nl)

**Abstract:** We present the development of Ag/Ge based ohmic contacts to n-type InP with both low contact resistances and relatively low optical losses. A specific contact resistance as low as  $1.5 \times 10^{-6} \Omega \text{ cm}^2$  is achieved by optimizing the Ge layer thickness and annealing conditions. The use of Ge instead of metal as the first deposited layer results in a low optical absorption loss in the telecommunication wavelength range. Compared to Au based contacts, the Ag based metallization also shows considerably reduced spiking effects after annealing. Contacts with different lengths are deposited on top of InP membrane waveguides to characterize the optical loss before and after annealing. A factor of 5 reduction of the propagation loss compared to the conventional Au/Ge/Ni contact is demonstrated. This allows for much more optimized designs for membrane photonic devices.

© 2015 Optical Society of America

**OCIS codes:** (130.3130) Integrated optics materials, (160.3900) Metals.

---

## References and links

1. M. Smit, J. van der Tol, and M. Hill, "Moore's law in photonics," *Laser & Photon. Rev.* **6**(1), 1–13 (2012).
2. J. van der Tol, R. Zhang, J. Pello, F. Bordas, G. Roelkens, H. Ambrosius, P. Thijs, F. Karouta, and M. Smit, "Photonic integration in indium-phosphide membranes on silicon," *IET Optoelectron.* **5**(5), 218–225 (2011).
3. V. Dolores-Calzadilla, D. Heiss, A. Fiore, and M. Smit, "Waveguide-coupled nanolasers in III-V membranes on silicon," in 15th International Conference on Transparent Optical Networks (ICTON), (2013), paper We.D6.1.
4. A. G. Baca, F. Ren, J. C. Zolper, R. D. Briggs, and S. J. Pearton, "A survey of ohmic contacts to III-V compound semiconductors," *Thin Solid Films* **308–309**, 599–606 (1997).
5. D. G. Ivey, D. Wang, D. Yang, R. Bruce, and G. Knight, "Au/Ge/Ni ohmic contacts to n-type InP," *J. Electron. Mater.* **23**(5), 441–446 (1994).
6. A. D. Rakic, A. B. Djuricic, J. M. Elazar, and M. L. Majewski, "Optical properties of metallic films for vertical-cavity optoelectronic devices," *Appl. Opt.* **37**(22), 5271–5283 (1998).
7. F. Ou, D. B. Buchholz, F. Yi, B. Liu, C. Hseih, R. P. H. Chang, and S.-T. Ho, "Ohmic contact of cadmium oxide, a transparent conducting oxide, to n-type indium phosphide," *ACS Appl. Mater. & Interfaces* **3**(4), 1341–1345 (2011).
8. Logeeswaran VJ, N. P. Kobayashi, M. S. Islam, W. Wu, P. Chaturvedi, N. X. Fang, S. Y. Wang, and R. S. Williams, "Ultrasoft silver thin films deposited with a germanium nucleation layer," *Nano Lett.* **9**(1), 178–182 (2009).
9. V. Dolores-Calzadilla, D. Heiss, and M. Smit, "Highly efficient metal grating coupler for membrane-based integrated photonics," *Opt. Lett.* **39**(9), 2786–2789 (2014).
10. W. Zhao, L. Wang, and I. Adesida, "Electrical and structural investigations of Ag-based ohmic contacts for InAlAs/InGaAs/InP high electron mobility transistors," *Appl. Phys. Lett.* **89**(7), 072105 (2006).

11. G. S. Marlow and M. B. Das, "The effects of contact size and non-zero metal resistance on the determination of specific contact resistance," *Solid-State Electron.* **25**(2), 91–94 (1982).
  12. L. Shen, Y. Jiao, L. Augstin, K. Sander, J. van der Tol, H. Ambrosius, G. Roelkens, and M. Smit, "A low-resistance spiking-free n-type ohmic contact for InP membrane devices," in *26th International Conference on Indium Phosphide and Related Materials (IPRM)*, (2014), pp. 1-2.
  13. Y. Jiao, J. Pello, A. M. Mejia, L. Shen, B. Smalbrugge, E. J. Geluk, M. Smit, and J. van der Tol, "Fullerene-assisted electron-beam lithography for pattern improvement and loss reduction in InP membrane waveguide devices," *Opt. Lett.* **39**(6), 1645–1648 (2014).
  14. Photon Design, FIMMWAVE, <http://www.photond.com>.
  15. A. H. Clark, "Electrical and Optical Properties of Amorphous Germanium," *Phys. Rev.* **154**(3), 750–757 (1967).
- 

## 1. Introduction

The ever-growing demand in data transport networks has promoted the development of high-density high-speed photonic integrated circuits [1]. Recently photonic membrane technologies, like the InP-Membrane-on-Silicon (IMOS) platform [2], attract significant attention. Thanks to the high refractive index contrast, these technologies provide novel solutions for fabricating devices with small volume, low power consumption and high bandwidth [3]. On the other hand, developments of new processing technologies are necessary for these novel membrane based high-performance devices.

Ohmic contacts on top of the membrane is one of the technologies that need to be optimized for electrically-pumped membrane opto-electronic devices. Firstly, devices with ever-smaller sizes require minimized specific contact resistances to obtain high speed and low power consumption. Secondly, in a photonic membrane, which is typically below one micron thick, the guided optical modes can be very close to the metal contacts on top, thereby resulting in higher optical losses. Traditional solutions include either designing a thick cladding layer as a buffer between the contact and active layers, or placing the contact away from the top of the device. However, these will not only increase processing complexities but also increase electrical and thermal series resistances. Hence, an ohmic contact with minimized optical loss is of great importance for membrane devices. The ohmic contact on top of a membrane device is typically n-type. This is because with Metalorganic Chemical Vapor Deposition (MOCVD) InP wafers are usually grown from n-side to p-side to avoid the diffusion of Zn (the p-type dopant). After flip-chip bonding and substrate removal, the n-type contact is deposited on top of the device structure. The n-type ohmic contact is therefore the focus of this work.

Au/Ge based n-type ohmic contacts are widely used in electronic devices based on III-V materials due to their low contact resistances after annealing [4]. However, the annealing process also leads to metal spiking as a result of Au diffusion at high temperatures. When it comes to membrane photonic devices, the spiking of metals into the semiconductor layers underneath can cause high optical losses and large leakage currents. A more advanced solution involves Ni as the first deposited layer for its ability to consume native oxides and the possibility of forming compounds at the InP surface with a lower barrier height [5]. To our knowledge, this optimized contact holds the lowest resistance level and is still being used in many InP based devices. However, the high optical absorption of Ni (546100 /cm at 1550 nm [6]) will limit its use in membrane photonic devices. Recent developments on transparent conducting oxides (TCO) provide low absorption ohmic contacts to n-type InP [7]. However the relatively high contact resistance and the complicated deposition process make it a non-ideal choice.

Ag is a widely used metal in plasmonic devices due to its very low optical loss. It can be deposited with an adhesion layer, like Ge, to different substrates [8, 9]. The significantly lower optical absorption of Ge at 1550 nm compared to that of conventionally used metal adhesion layers (like Ni, Ti or Cr) promises low loss contacts. Furthermore, Ge also contributes to the n-type doping of the semiconductors, thereby reducing the contact resistance [4]. It has been

shown in high electron mobility transistors (HEMTs) that Ag/Ge based ohmic contacts can provide contact resistances as low as those from Au/Ge based ones. Moreover, the thermal stability is also improved compared to Au/Ge systems due to a much higher eutectic phase temperature of the Ag/Ge alloy [10].

In this paper, we investigate these potential advantages of Ag/Ge as a new ohmic contact solution for InP-membrane based photonic devices. A standard metal deposition process is used and no special surface treatments are required. The specific contact resistance is optimized to approach the level of  $10^{-6} \Omega \text{ cm}^2$ . We compare the interfaces of InP with different contacts. In contrast to Au/Ge/Ni, no spiking of Ag/Ge into the InP layer is observed after 400 °C annealing. Finally, the optical losses from different contacts are demonstrated with membrane waveguides. The Ag/Ge based contacts show the lowest propagation loss both before and after annealing. In addition, the effects of Ge on the contact resistance and the optical loss are discussed.

## 2. Specific contact resistance

The specific contact resistance of Ag/Ge is characterized using the circular transfer length method (CTLM) [11]. The samples used in this test come from a Fe-doped semi-insulating InP (100) substrate. A 100 nm thick n-InP contact layer is grown on top of the substrate with MOCVD. This n-InP layer is doped by Si to a level of  $2 \times 10^{18} \text{ cm}^{-3}$ . Prior to metal deposition, the samples are cleaned in an oxygen plasma (50 W, 5 minutes), followed by dipping in a  $\text{H}_3\text{PO}_4:\text{H}_2\text{O}$  (1:10) solution for 2 minutes. After these treatments, a layer of Ge is deposited on top of the n-InP layer with electron beam evaporation, followed by the deposition of 300 nm of Ag. Four samples with different thicknesses of the Ge layer are processed. Each sample is cleaved into several parts to test different annealing temperatures. The annealing is performed with a rapid thermal process in  $\text{N}_2$  ambient for 15 seconds.

Fig. 1 shows the CTLM results on the specific contact resistances as a function of the annealing temperatures. Before annealing, only the sample with 2 nm of Ge shows ohmic behavior. We attribute this to a sufficiently strong tunneling effect with such a thin Ge layer. All of the samples show ohmic behavior after annealing at 300 °C and their resistances reduce further by increasing the temperature. The optimal range lies between 350 °C to 400 °C. Annealing at 450 °C leads to increases of the contact resistance, which is assumed to be related to interface degradations at higher temperature [10]. The effect of the Ge thickness on the contact resistance can be seen in these plots. Ge is supposed to increase the doping of the top surface of the n-InP layer after annealing, thereby reducing the contact resistance. In our experiments, this is seen for the annealed samples with 15 or 30 nm of Ge, which provide much lower contact resistances compared to those with only 2 nm of Ge. Thicker Ge (50 nm) however does not give further improvements. It is likely that only a certain amount of Ge can diffuse and contribute to the doping during annealing [5]. The lowest specific contact resistance of  $1.5 \times 10^{-6} \Omega \text{ cm}^2$  is obtained from the samples with 30 nm of Ge and a 400 °C annealing. This value makes this ohmic contact suitable for a wide range of applications.

## 3. Annealed contact interface

In order to check the contact-InP interface and the spiking effect due to annealing, scanning electron microscope (SEM) cross-sectional images are taken on focused ion beam (FIB) cut facets. Contacts are deposited on an InP test wafer consisting of a n-InP contact layer (100 nm) and a InGaAs layer (200 nm). Fig. 2(a) shows the interface of InP and the optimized Ag/Ge contact (30 nm Ge, 400 °C annealing). A few spikes of Ag into the Ge layer can be seen. They all stop at the interface to InP. Those spikes may be important in reducing the contact resistance as studied in a HEMT structure [10]. As they do not penetrate further into the semiconductor layers, limited influence on the optical modes guided in those layers can be expected. As a

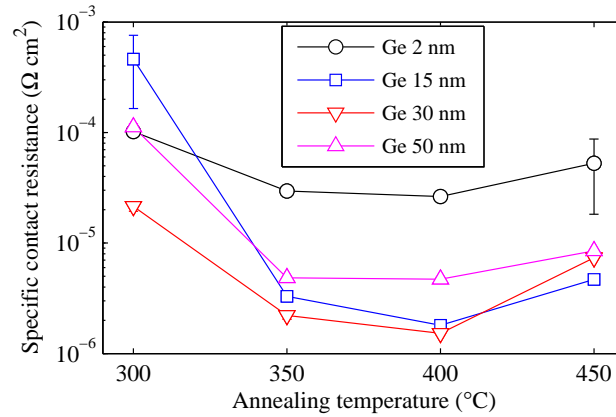


Fig. 1. Specific contact resistance of Ag/Ge contacts as a function of annealing temperature. Samples with various thicknesses of Ge are shown.

comparison, the conventional Au/Ge/Ni (250/50/30 nm) contact on the same semiconductor layers is shown in Fig. 2(b). It is annealed at the same temperature (400 °C). Such a metal-stack, together with this annealing condition, has been tested to provide ultra-low contact resistances ( $<10^{-6} \Omega \text{ cm}^2$ ) to n-InP [5, 12]. In contrast to the Ag/Ge contact, the interface is much rougher here. The 100 nm n-InP layer is completely penetrated. Some of the spikes can even penetrate up to 300 nm, through the InGaAs layer. Such a strong diffusion is believed to result from the liquid phase of the Au/Ge alloy [10]. Its eutectic temperature (361 °C) is lower than the optimal annealing temperature (400 °C), leading to the well-known spiking effects for Au/Ge based contacts used in electronic devices. In fact, the spiking effect has been observed even at temperature lower than 361 °C [5, 10]. When it comes to optical devices, the higher eutectic temperature (651 °C) of the Ag/Ge alloy makes it a superior contact solution with much less spiking effects into the device layers.

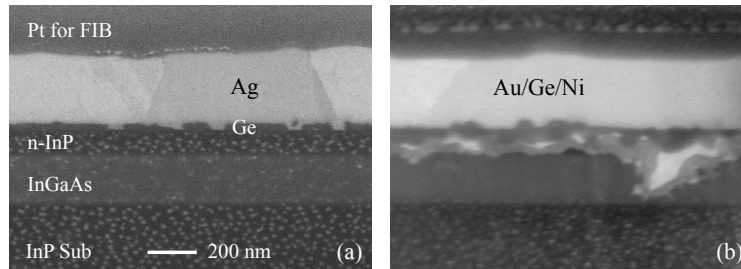


Fig. 2. Cross-sectional SEM images of annealed (a) Ag/Ge and (b) Au/Ge/Ni contacts to n-InP. Both are annealed at 400 °C for 15 s.

#### 4. Waveguide loss measurements

Since the SEM images are taken at a limited number of locations of the samples, they can only provide local information about the spiking effects. In order to evaluate the overall influence of the contact on the optical characteristics of integrated photonic devices, straight InP based membrane waveguides (WGs) are fabricated for optical loss measurements [see Fig. 3(a)]. They are fabricated in the IMOS platform. A detailed description of the process flow can be found

elsewhere [13]. Afterwards, contacts with different lengths are patterned on top of the WGs using electron beam lithography and a lift-off process. The widths of the WGs and the contacts are designed as  $10\ \mu\text{m}$  and  $7\ \mu\text{m}$ , respectively, to avoid metal covering the side-wall of the WGs [see Fig. 3(b)]. Fig. 3(c) shows the cross-section of the structure. The thickness of the WGs is chosen as  $300\ \text{nm}$  so that in the vertical direction only one guided mode can propagate. In the measurement, the light from a laser working in the telecommunication wavelength range is coupled to the input grating coupler with a single-mode fiber. The transmitted light is coupled out from the output grating coupler to another fiber, and finally measured with a power meter. Both fibers are placed with an angle of  $9^\circ$  from the normal direction to the surface of the sample. The gratings are designed to couple in TE polarized light. All measurements are done at a wavelength of  $1550\ \text{nm}$ .

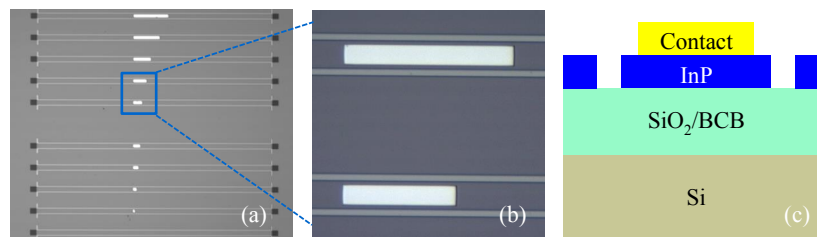


Fig. 3. (a) Image of an array of fabricated membrane WGs. The dark parts at both ends of each WG are the grating couplers (b) Zoom-in image of two contacts on top of the WGs. (c) Cross-section of the WG with contact on top.

Fig. 4(a) shows the insertion loss (including both propagation loss and grating coupling loss) measured just after contact deposition without annealing. Three different contacts have been measured: Ag/Ge ( $300/30\ \text{nm}$ ), Au/Ge ( $250/50\ \text{nm}$ ) and Au/Ge/Ni ( $250/50/30\ \text{nm}$ ). The measured data is fitted with a linear function to extract the loss coefficient of the propagation through the contact section [see Table. 1]. Owing to the high absorption of Ni, conventional Au/Ge/Ni contacts show a much higher loss compared to the other two contacts. Au and Ag are both known as low-loss metals due to their low refractive indices and the corresponding small confinements of the mode field. The lower loss coefficient of Ag/Ge as compared to that of Au/Ge can be attributed to the relatively lower absorption of Ag and a slightly thinner layer of Ge in that contact. In order to evaluate the Ge loss, simulations are performed [14] to calculate the material absorption of Ge based on the resultant loss coefficients from Ag/Ge and Au/Ge and the WG structures. Only the fundamental mode propagating in the WG is considered in this simulation. The as-deposited contact layers are assumed to be uniform. Literature parameters of Au and Ag are used [6]. The refractive index of Ge is assumed to be  $4.3$  [14]. From the simulation, the material absorption coefficient of Ge is calculated to be around  $5000\ \text{/cm}$ . Most simulators use a smaller value (typically lower than  $1000\ \text{/cm}$  at  $1550\ \text{nm}$ ) which is based on measurement data of crystalline Ge. It can be expected that the deposited amorphous Ge has a higher absorption coefficient depending on the evaporation conditions [15]. Nevertheless, this measured absorption coefficient of Ge is still orders of magnitude lower than those of the metals that are conventionally used as the first deposited layer in ohmic contacts.

Fig. 4(b) shows the insertion loss measured after the annealing. Two arrays of WGs of each contact have been measured. All contacts give an increased loss after annealing. The data points become more scattered, particularly in Au based contacts, indicating the random and localized effects of the spiking. The loss of the Au/Ge contact, which was close to the value of Ag/Ge before annealing, increases dramatically and almost reaches the level of Au/Ge/Ni. This seems to indicate that compared to Ni absorption, random scattering losses become more dominant in the

WGs with strong metal spiking and rough interfaces. Hence, the linear fitting for extracting the loss coefficients may be less meaningful. Nevertheless, an obvious difference (approximately a factor of 5) of the loss between the annealed Ag and Au based contacts is observed.

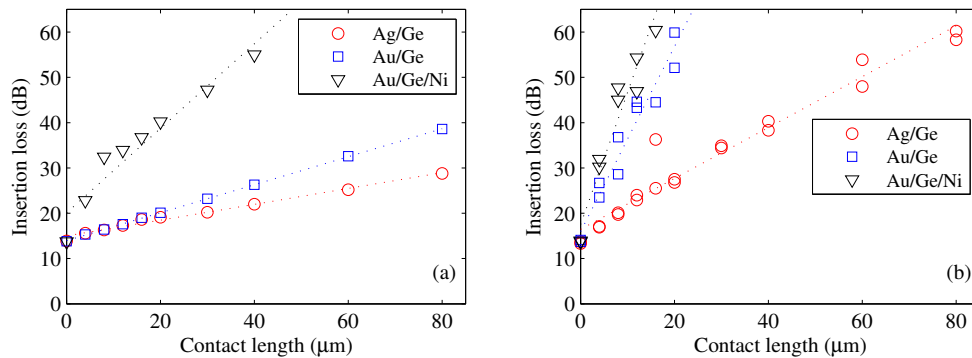


Fig. 4. Insertion loss of membrane WGs as a function of contact length. Results with different contacts are shown. Dotted lines represent linear fits. (a) Measured before annealing. (b) Measured after annealing at 400 °C for 15 s.

Table 1. Fitted loss coefficients (dB/μm).

Contact type	Before annealing	After annealing
Ag/Ge	0.175	0.562
Au/Ge	0.309	2.044
Au/Ge/Ni	0.934	2.911

The increase of loss of the annealed Ag/Ge contact may be related to the spikes in the Ge layer observed in Fig. 2(a). The optical mode propagating in such a thin membrane WG has a substantial overlap with the interfacial layers. As a consequence, those spikes, even though they stop on top of the WG layer, can still cause a notable increase of the loss. Diffusion of Ge into the n-InP layer after annealing can be another reason for the increase of the loss. This diffusion is not observed in the SEM image, but can be deduced from the electrical measurements.

## 5. Conclusion

We have developed a new n-type ohmic contact for InP membrane photonic devices. This Ag/Ge based contact provides a specific contact resistance as low as  $1.5 \times 10^{-6} \Omega \text{ cm}^2$  after a 15 s annealing at 400 °C. The annealed contacts show much more uniform interfaces and much less spiking effects compared to Au based contacts. Membrane waveguide loss measurements show a factor of 5 difference in the propagation loss between Ag/Ge contacts and conventional Au/Ge/Ni contacts. These superior properties in both electrical and optical behavior promise more optimized designs for membrane photonic circuits and for plasmonic devices.

## Acknowledgments

This work is supported by the ERC project NOLIMITS and the EU FP7 project NAVOLCHI. The authors acknowledge Nanolab@TU/e for the cleanroom facilities. LS thanks B. Barcones Campo, E.J. Geluk, S.P. Bhat and P.J. van Veldhoven for technical supports.